Publication Year	2019
Acceptance in OA	2021-01-28T10:59:45Z
Title	Characterization of the Murchison Widefield Array Dipole with a UAV-mounted Test Source
Authors	Fabio Paonessa, Lorenzo Ciorba, Giuseppe Virone, BOLLI, Pietro, MONARI, JADER, PERINI, FEDERICO, Randall Wayth, Adrian Sutinjo, David Davidson
Handle	http://hdl.handle.net/20.500.12386/30071

Characterization of the Murchison Widefield Array Dipole with a UAV-mounted Test Source

Fabio Paonessa[1], Lorenzo Ciorba[1], Giuseppe Virone[1], Pietro Bolli[2], Jader Monari[3], Federico Perini[3], Randall Wayth[4], Adrian Sutinjo[4], David Davidson[4]

[1] Istituto di Elettronica e di Ingegneria dell'Informazione e delle Telecomunicazioni (IEIIT), Consiglio Nazionale delle Ricerche (CNR), Turin, Italy, giuseppe.virone@ieiit.cnr.it

[2] Osservatorio Astrofisico di Arcetri (OAA), Istituto Nazionale di Astrofisica (INAF), Florence, Italy

[3] Istituto di Radioastronomia (IRA), Istituto Nazionale di Astrofisica (INAF), Bologna, Italy

[4] International Centre for Radio Astronomy Research (ICRAR), Perth, Australia

***Abstract*—Aperture arrays such as the Australian Murchison Widefield Array (MWA) represent the modern approach to low frequency radio astronomy. The presence of mismatched front-end amplifiers and mutual coupling between the array elements produce distortions in the embedded-element patterns. Advanced techniques are therefore required to perform the in-situ validation and instrumental calibration. Unmanned Aerial Vehicles (UAVs) technology provides suitable tools to accomplish these tasks. In preparation of possible UAV applications at the MWA site, some tests have been carried out in Italy on a subarray of MWA dipoles. This contribution presents the results of the measurement session with particular reference to the calibration of the measurement equipment.**

***Index Terms*—aperture arrays, radio astronomy, unmanned aerial vehicles.**

I. Introduction

Low Frequency Aperture Arrays (LFAAs) represent the new generation of radio telescopes aimed at studying key science such as the epoch of reionization and the cosmic dawn [1]. The Murchison Widefield Array (MWA) [2] in Australia and the Low Frequency Array (LOFAR) [3] in Europe are two examples of operating facilities. They also represent pathfinders/precursors for the future LFAA of the Square Kilometre Array (SKA) [4]. The MWA in particular is located at the Murchison Radio-astronomy Observatory (MRO) in Western Australia, the planned site of the future SKA1-Low.

As accurately analyzed in [5], the mutual coupling between the array elements and the presence of mismatched active components such as Low Noise Amplifiers (LNAs) can produce distortions in the embedded-element patterns (EEPs) that complicate the instrument calibration process. Finite ground planes and soil parameters produce additional uncertainty. The characterization of the antennas in their operative condition is therefore required [6]. For this purpose, a measurement approach using an Unmanned Aerial Vehicle (UAV) has been developed in Italy since 2014 [7]. Several activities on array prototypes [8–10] and operating facilities [5, 11] have been carried out. Near-field verification techniques have also been proposed to deal with very large arrays for which the far-field distance cannot be easily satisfied [11].

Within the collaboration between the Australian team (International Centre for Radio Astronomy Research, ICRAR) and the Italian one (National Institute for Astrophysics, INAF, and National Research Council, CNR), the flying test source has been recently used to characterize the embedded-element patterns of the MWA dipole with two adjacent elements (see Figs. 1a and 1b), at the frequencies of 50, 150, 250 and 350 MHz. A specific calibration strategy has been implemented in order to improve the accuracy of the measured data. Relevant results of this experimental campaign are presented in the paper.

(a)

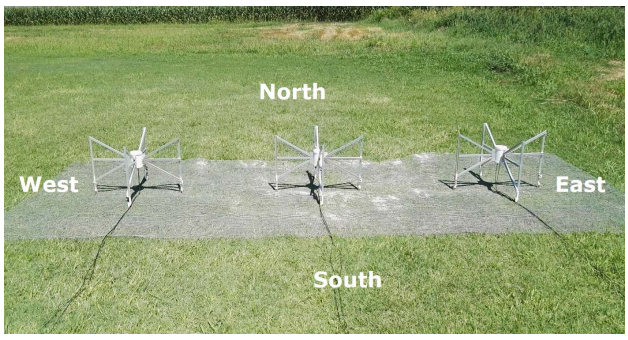

(b)

Fig. 1. (a) the UAV equipped with the RF generator and the dipole antenna, (b); the MWA dipoles over a 5×2 m^2 ground plane at the measurement site in Italy.

II. Experimental Results

The MWA consists of 2048 dual-polarization dipole antennas arranged in 128 tiles of 4×4 elements. A set of MWA antennas has been shipped to Italy. Three elements have been assembled in a linear array to characterize the embedded-element patterns (see Fig. 1b). The array has been placed over a 5×2 m^2 grid ground plane. The mesh size of 1.25 cm was definitely smaller than the wavelength at all the considered frequencies. The distance between each element was 1.55 m (center-to-center). This layout (spacing and orientation) is consistent to the diagonal of an MWA tile.

According to Fig. 2, each LNA output was connected to a 7-m-long KSR100 coaxial cable. Each cable was in turn connected to the RF+DC port of a bias tee. The RF port corresponding to the central element was connected to a spectrum analyzer through a low-loss 60-m LMR400 coaxial cable. All the six LNAs were powered-up. The RF ports of the bias tees not connected to the spectrum analyzer were terminated with matched loads. The absence of RFI and the linearity of the LNAs have been verified at the measurement site in the operative conditions.

The micro UAV already used in [12] (maximum take-off mass within 4 kg, see picture in Fig. 1a) was equipped with a tunable RF generator and a tunable dipole antenna to operate as a far-field flying test source. An onboard real-time differential GPS provided centimeter-level-accurate position data to the flight control board, improving the flight performance. According to [13], the distance between the dipole and the UAV frame has been adjusted in order to avoid significant pattern distortions produced by the resonance of the UAV metal frame at the operative frequencies.

Fig. 3 shows the measured and simulated normalized embedded-element patterns of the central MWA dipole at the frequencies 50, 150, 250 and 350 MHz. All the curves are normalized at zenith. Each pattern has been measured by means of a rectilinear flight above the array at a constant height of 70 m. The far-field condition is approximately 58 m at 350 MHz. The shown patterns refer to the MWA dipole oriented along the north-south direction (see Fig. 1b), named y-polarization. The simulations have been performed with FEKO, and the LNA impedance has been extracted from [14]. The overall agreement is good and the discrepancy is mostly within 0.5 dB.

At 50 MHz (Fig. 3a), the electrically short dipole used on the UAV [15] is highly mismatched, reducing the overall radiated power. The MWA active dipole also has a very limited gain at this frequency (lower frequency of MWA is 80 MHz). Therefore, the noise floor of the measurement equipment (Agilent E4402B spectrum analyzer) impacts the measurement accuracy for high values of zenith angle. The spectrum analyzer was configured in zero-span mode and 10 kHz resolution bandwidth, which gives 80 dB of dynamic range.

The localized fast ripples in the measurements are mainly related to residuals of the compensation for the variable UAV attitude (i.e. spatial orientation) [16].

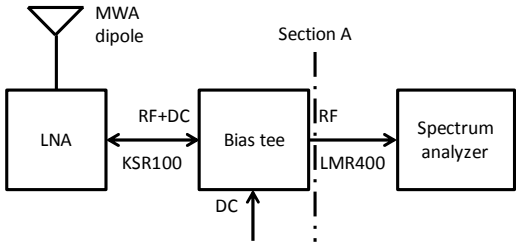

Fig. 2. Connection of one MWA dipole. Section A identifies the location where the test-source signal is injected to the spectrum analzer for reference measurements.

The asymmetry in the measured pattern at 350 MHz can be produced by both the mechanical uncertainties in the antenna-under-test assembly with particular reference to the flatness of the ground plane and the reduced phase balance between the two inputs of the differential LNA (MWA upper frequency is 300 MHz).

In [15], the antenna gain was obtained from the measured received power by means of an accurate characterization of all the contributions in the RF chain (e.g. transmitted power, cables attenuation etc.). In this paper, a different approach has been used. With reference to Fig. 2, the output of the RF generator on the UAV has been directly connected to the LMR400 cable (going to the spectrum analyzer) in place of the output RF port of the bias-tee (section A in Fig. 2). This condition represents a reference measurement P_{ref} that is exploited to calibrate out several error contributions, including the power generated by the frequency generator. In particular, the AUT gain at zenith is computed as follows

$$g_{AUT} = P_{rec} + IL + ML - g_{UAV} + PL - P_{ref} \qquad (1)$$

where all the quantities are expressed in decibels. P_{rec} is the measured received power, IL is the insertion loss of the onboard balun, ML is the loss due to the reflection coefficient of the dipole antenna on the UAV, g_{UAV} is the gain of the test-source (simulated according to [13]) and PL is the path loss. It should be noted that the contributions of the generated RF power and the LMR400 cable losses do not explicitly appear in (1), therefore their knowledge is not required. Moreover, the difference between P_{rec} and P_{ref} cancels out the spectrum analyzer amplitude error. According to the error contributions reported in [15], the estimated measurement accuracy (1σ) is approximately ±0.82 dB at 50 MHz and ±0.14 dB at the other frequencies.

Table I shows the measured and simulated active-element gain at zenith. It includes the gain of both the antenna (y-polarization only) and the LNA [17], and the losses of KSR100 cable and bias tee (known from characterization). The simulation at 50 MHz has not been included owing to the large impedance mismatch of the antenna. The consistency between measurement and simulation is very good at 150 MHz. The larger discrepancy at higher frequencies could be reduced by refining the simulation as far as the interaction between antenna and LNA is concerned.

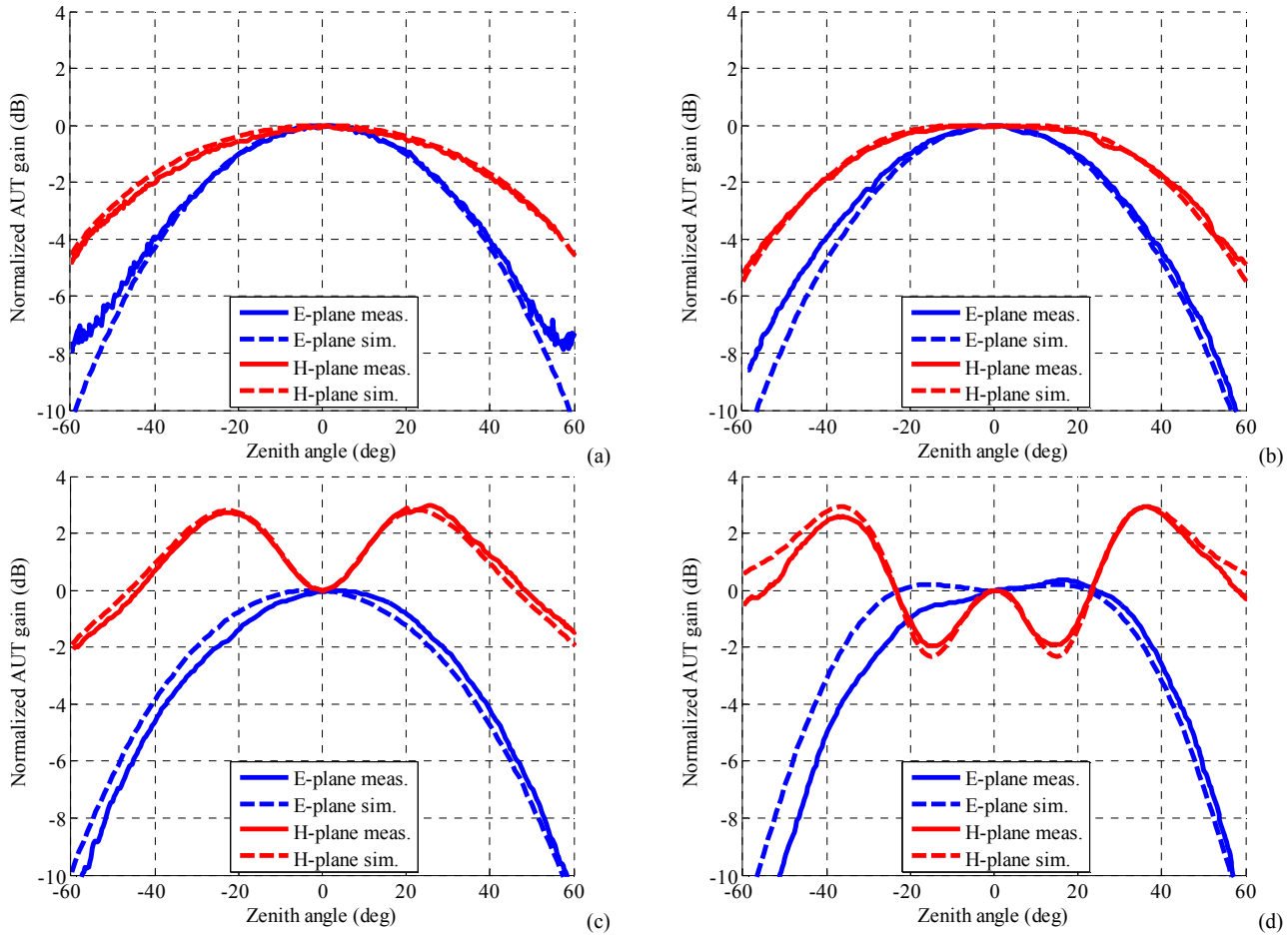

Fig. 3. Measured (solid lines) and simulated (dashed lines) normalized embedded-element patterns for the y-polarization of the central element (oriented along the north-south direction, see Fig. 1b). Blue color for the E-plane cuts, red for the H-plane ones. (a) 50 MHz, (b) 150 MHz, (c) 250 MHz, (d) 350 MHz.

III. CONCLUSION

The presented results obtained on a subarray of three MWA dipoles at different frequencies from 50 MHz to 350 MHz are in good agreement with the simulated response of the central embedded element. The adopted calibration strategy yields to a good measurement accuracy and can be easily implemented on the measurement field for future test campaigns both in the case of an MWA tile and in the case of a larger SKA1-Low station.

ACKNOWLEDGMENT

The authors thank Augusto Olivieri (CNR-IEIIT) for his valuable technical support.

TABLE I. MEASURED AND SIMULATED AUT GAIN AT ZENITH

	AUT gain (dBi)	
Frequency (MHz)	***Measured***	***Simulated***
50	-17.2	NA
150	25.2	24.9
250	21.1	23.5
350	20.1	22.2

REFERENCES

[1] L.V.E Koopmans et al., "The Cosmic Dawn and Epoch of Reionization with the Square Kilometre Array," SKA Science Book 'Advancing Astrophysics with the Square Kilometre Array', PoS(AASKA14)001, May 2015.

[2] M. P. van Haarlem et al., "LOFAR: The LOw-Frequency ARray," Astronomy & Astrophysics, 556, A2, August 2013

[3] S. J. Tingay et al., "The Murchison Widefield Array: The Square Kilometre Array Precursor at Low Radio Frequencies," Publications of the Astronomical Society of Australia, 30, 7, January 2013

[4] P. E. Dewdney et al., "The Square Kilometre Array," Proceedings of the IEEE, 97, 8, August 2009

[5] G. Virone et al., "Strong Mutual Coupling Effects on LOFAR: Modeling and In Situ Validation," IEEE Transactions on Antennas and Propagation, vol. 66, no. 5, pp. 2581-2588, May 2018. DOI: 10.1109/TAP.2018.2816651

[6] A. T. Sutinjo et al., "Characterization of a low-frequency radio astronomy prototype array in Western Australia," IEEE Trans. Antennas Propag., vol. 63, no. 12, pp. 5433–5442, Dec. 2015.

[7] G. Virone et al., "Antenna Pattern Verification System Based on a Micro Unmanned Aerial Vehicle (UAV)," IEEE Antennas and Wireless Propagation Letters, vol. 13, pp. 169-172, 2014. DOI: 10.1109/LAWP.2014.2298250

[8] G. Pupillo et al., "Medicina Array Demonstrator: calibration and radiation pattern characterization using a UAV-mounted radio-frequency source," Experimental Astronomy, vol. 39, issue 2, pp. 405-421, June 2015. DOI: 10.1007/s10686-015-9456-z

[9] P. Bolli et al., “From MAD to SAD: the Italian experience for the Low Frequency Aperture Array of SKA1-LOW”, Radio Science, vol. 51, issue 3, pp. 160–175, Mar. 2016. DOI: 10.1002/2015RS005922

[10] E. de Lera Acedo et al., “SKA Aperture Array Verification System: Electromagnetic modeling and beam pattern measurements using a micro UAV”, Experimental Astronomy, vol. 45, issue 1, pp. 1–20, Mar. 2018. DOI: 10.1007/s10686-017-9566-x

[11] P. Bolli et al., “Near-Field Experimental Verification of the EM Models for the LOFAR Radio Telescope,” IEEE Antennas and Wireless Propagation Letters, vol. 17, issue 4, pp. 613–616, Apr. 2018. DOI: 10.1109/LAWP.2018.2859828

[12] F. Paonessa et al., “UAV-Mounted Corner Reflector for in-Situ Radar Verification and Calibration,” 2018 IEEE Conference on Antenna Measurement and Applications (CAMA 2018), Västerås, Sweden, Sept. 3-6, 2018

[13] F. Paonessa et al., “UAV-Based Antenna Measurements: Improvement of the Test Source Frequency Behavior,” 2018 IEEE Conference on Antenna Measurement and Applications (CAMA 2018), Västerås, Sweden, Sept. 3-6, 2018

[14] D. Ung, “Embedded Element Pattern Beam Model for Murchison Widefield Array,” 2016 [Webinar]

[15] P. Bolli et al., “Antenna pattern characterization of the low-frequency receptor of LOFAR by means of an UAV-mounted artificial test source,” SPIE Ground-based and Airborne Telescopes VI, Edinburgh, Scotland, United Kingdom, June 26 – July 1 2016. DOI 10.1117/12.2232419

[16] F. Paonessa et al., “Effect of the UAV orientation in antenna pattern measurements,” European Conference on Antennas and Propagation (EuCAP), Lisbon, Portugal, Apr. 12-17 2015

[17] B. Juswardy, “Comparison of Broadcom ATF-54143 vs SAV-541 for MWA LNA”, 2018 [ICRAR internal report]